# Facile electrochemical synthesis, using microemulsions with ionic liquid, of highly mesoporous CoPt nanorods with enhanced electrocatalytic performance for clean energy

*A. Serrà, E. Gómez, E. Vallés*[*]

*Grup d'Electrodeposició de Capes Primes i Nanoestructures (Ge-CPN), Departament de Química Física and Institut de Nanociència i Nanotecnologia (IN*$^2$*UB), Universitat de Barcelona, Martí i Franquès 1, E-08028 Barcelona, Catalonia (Spain)*

***Abstract***

We have established a facile and generalizable electrochemical synthesis of metallic mesoporous nanorods in the nanochannels of commercial polycarbonate membranes using microemulsions containing ionic liquids. Herein, we report the preparation of magnetic CoPt nanorods with various meso or nanopores distributions, depending on the microemulsion type (ionic liquid –in-water (IL/W), bicontinuous (β) or water-in-ionic liquid (W/IL)). The synthesized porous nanorods show a much enhanced electrocatalytic activity for methanol oxidation in comparison with compact Pt nanorods (up to 12 times) or Pt/C electrocatalyst (Pt nanoparticles or commercial black platinum). Therefore, the synthesized CoPt mesoporous nanorods could be excellent catalysts in direct methanol fuel cells (DMFC's), as they have high surface areas, large pore volumes and high corrosion stability, and they exhibit promising catalytic properties.

**Highlights**

- Highly mesoporous CoPt nanorods for electro-oxidation of methanol in fuel cells

- Much better performance than usual platinum catalysers
- A facile electrochemical approach of synthesis of highly mesoporous nanorods
- Microemulsions containing ionic liquids as synthesis medium of the nanostructures

**Keywords**

Methanol electro-oxidation, catalysts for fuel cells, CoPt nanorods, mesoporous nanorods, electrodeposition, microemulsions

## 1. Introduction

In the past decade, a wide range of proposals have been devoted to synthesizing different nanomaterials as nanoparticles [1-3] or nanorods [4-6], due to their potential applications, particularly in the areas of catalysis, adsorption, fuel cells and biomaterials.

Nowadays, nanomaterials arouse an enormous interest as regards in energy conversion and storage devices, due to their effectiveness as electrocatalysts for Methanol (DMFCs) or Ethanol (DEFCs) Fuel Cells [7, 8]. However, the disadvantages of the high cost and low supply of Pt-based catalysts, the crossover effect, as well as their poor durability, seriously limit their commercial availability. Currently, significant improvements in the DMFCs have been made by combining different tactics, but several problems still remain unsolved. The major advances focus on enhancing their durability and their electrocatalytic activity by increasing both the surface – volume ratio and the catalytic performance [9-12].

The use of nano or mesoporous structures has been proved to be an effective approach to lowering the loading of Pt and improving its catalytic activity as a consequence of their high surface-volume ratio. Mesoporous nanomaterials can be prepared through several methodologies including the traditional hard-templating [13, 14], phase separation [15, 16] and alloy-dealloying approaches [17-19], amongst others. In the last years, soft-template systems like liquid crystals have been proposed as a new synthetic route [20-23]. Nevertheless, these approaches are not very simple enough, so trying to find new facile and successful pathways to produce nano or

mesoporous nanomaterials of metals and alloys has become a new challenge in the fabrication of nanocatalysts.

Recently, surfactant micelles have been demonstrated as a useful tool to synthesizing mesoporous Pt nanorods in the confined space of polycarbonate membranes [24]. This method, however, has only been used to fabricate platinum nanorods with a single pore size and in very specific conditions.

The preparation of bimetallic platinum catalysts with 3d-transition metals (Fe, Co, Ni, among others) is another widely applied strategy to enhance the electrochemical activity for methanol oxidation (reduction of poisoning by adsorbed intermediates) and to reduce the catalyst costs [25, 26].

Lastly, magnetic nanostructures have emerged as a new type of promising multi-functional architectures for potential applications in data storage, magnetic carriers for biomedical devices or magnetic catalysts [27, 28]. The manipulation and recyclability of the catalytic material would be easier with magnetic catalysts, because their magnetic behaviour facilitates the anchoring or recovery of the material by applying an external magnetic field [29, 30]. Magnetic CoPt alloys permits combining both characteristics. Moreover, the CoPt alloys are generally more stable than other platinum alloys (with Ni, Fe or V), due to the higher degree of alloying of the cobalt with the platinum [31, 32].

Herein we report a new, facile and successful approach for synthesising CoPt magnetic nano or mesoporous nanorods in a single pot. These are grown, by means of electrodeposition method, in the nanochannels of commercial polycarbonate membranes, using water-in-ionic liquid (W/IL) as well as bicontinuous (β) and ionic liquid-in-water (IL/W) microemulsions. The bimetallic nanostructures synthesized with this procedure show much enhanced activity, strong methanol tolerant capability and corrosion resistance in comparison with compact CoPt nanorods, commercial Pt/C catalysts or other recent state-of-the-art Pt-based nanostructures.

## 2. Experimental

### 2.1. Materials

Non-ionic surfactant p-octyl polyethylene glycol phenyl ether a.k.a. Triton X-100 (Acros Organics, 98%), ionic liquid 1-butyl-3-methylimidazolium hexafluorophosphate a.k.a bmim$PF_6$, Arcos Organics, >98%), chloroform (Sigma-Aldrich, +99 %), boric acid (Merck, 99.8%), Co(II) chloride (Carlo Erba, > 98.0%), sodium hexacloroplatinate(IV) hexahydrate (Aldrich, 98%), ammonium chloride (Fluka, > 99.5%), boric acid (Merck, 99.8%), and deionized water (Millipore Q-System) with a resistivity of 18.2 MΩ $cm^{-1}$.

### 2.2. Microemulsion Preparation

Microemulsions were prepared by mixing a CoPt aqueous solution (2.5 mM $CoCl_2$, 1.2 mM $Na_2PtCl_6$, 0.1 M $NH_4Cl$, 10 g·$dm^{-3}$ $H_3BO_3$ and pH = 4.5) (W), an ionic liquid (bmim$PF_6$) (IL) and a surfactant (Triton X-100 (p-octyl polyethylene glycol phenyl ether)) (S) at 25 ºC in different proportions, to define different kind of microemulsions. According to the bibliography [33], a 66.5 wt. % of water, 5.0 wt. % of bmim$PF_6$ and 28.5 wt. % of Triton X-100 forms an ionic liquid-in-water microemulsion (IL/W), a 55.8 wt. % of water, 7.0 wt. % of bmim$PF_6$ and 37.2 wt. % of Triton X-100 forms a bicontinuous microemulsion (β) and a 26.7 wt. % of water, 11.0 wt. % of bmim$PF_6$ and 62.3 wt. % of Triton X-100 forms a water –in-ionic liquid microemulsion (W/IL). We use these proportions for preparing the microemulsions, but substituting the pure water for the CoPt electrolytic solution. Electrodeposition will take place from the aqueous component of the microemulsion.

### 2.3. Electrosynthesis of CoPt Nanorods

20 µm-thick commercially available polycarbonate (PC) membranes (Millipore Co., USA) with 200 nm pore size diameter, metalized by sputtering with gold (100 nm-thick) on one side, were used to synthesize the nanorods. The electrochemical fabrication was performed at room temperature (25 ºC) using a three-electrode electrochemical system with a platinum wire, PC membrane, and an Ag/AgCl (3M KCl) electrode as counter, working and reference electrodes, respectively, by applying a constant potential of -1.05 V (controlled by potentiostat/galvanostat

Autolab with PGSTAT30 Equipment and GPES software) at 25 ºC. Prior to the electrodeposition, the PC membranes were immersed 12 h in the different media to assure a uniform filling of the pores.

### 2.4. Nanorods Characterization

In order to analyse the morphology and structure of the nanorods, the sputtered gold layer was etched with $I_2$/I- solution and the polycarbonate membrane was dissolved with chloroform and washed with chloroform (x3), ethanol (x3) and water (x2). The nanorods morphology was analysed by using Field-Emission Scanning Electron Microscopy (Hitachi 800 MT) and High-Resolution Transmission Electron Microscopy (Jeol 2100). An X-ray analyser incorporated in a Leica Stereo Scan S-360 Equipment was used to determine the elemental composition. Furthermore, to test the electrocatalytic activity for the methanol oxidation and the corrosion behaviour, a glassy carbon electrode was used as a support in which to deposit the nanorods by means of an ink with water and 5 wt. % of Nafion solution.

## 3. Results and discussion

The manufacturing procedure of the CoPt nanorods implies the electrodeposition of the CoPt in the interior of the channels of the polycarbonate membranes. Therefore, different CoPt nanorods (nano/mesoporous or compact as a reference) were synthesized using the pure CoPt aqueous solution (100% of aqueous component - W), and the three microemulsions, which are described in the Experimental Section:

- Ionic Liquid-in-Water microemulsion (IL/W): 66.5 wt. % of CoPt aqueous solution, 5.0 wt. % of bmim$PF_6$ and 28.5 wt. % of Triton X-100.
- Bicontinuous microemulsion (β): 55.8 wt. % of CoPt aqueous solution, 7.0 wt. % of bmim$PF_6$ and 37.2 wt. % of Triton X-100.
- Water-in-Ionic Liquid microemulsion (W/IL): 26.7 wt. % of CoPt aqueous solution, 11.0 wt. % of bmim$PF_6$ and 62.3 wt. % of Triton X-100.

In Figure 1a, the light areas of the cylinders represent the different synthesis media (the electroactive species are dissolved in the aqueous component in all the cases), with their nanostructure, whereas the dark areas represent the CoPt nanowires synthesized from each system. The three microemulsions used contain the same surfactant: ionic liquid ratio ($R_{S:IL}$) and a different CoPt solution percentage.

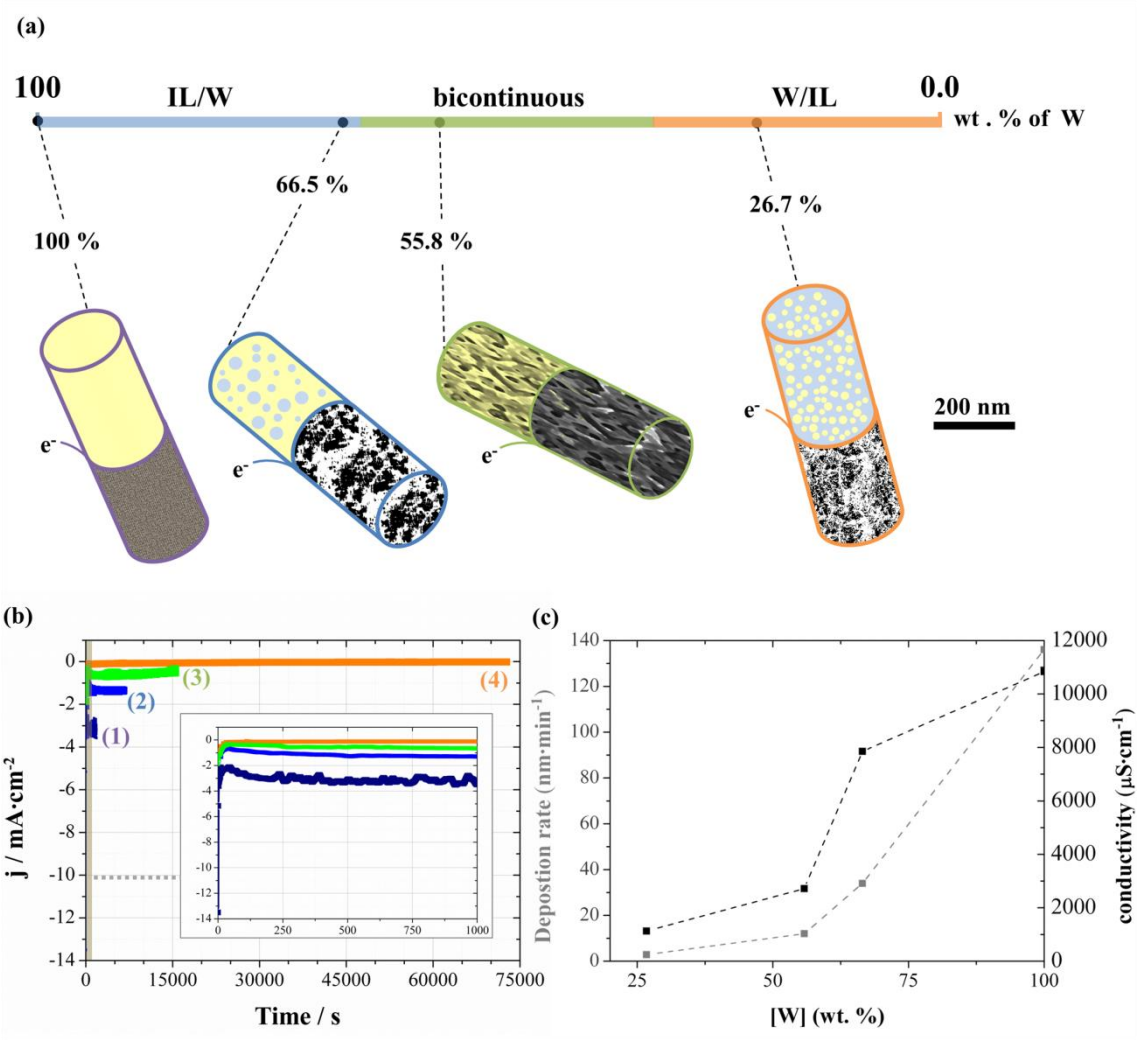


Figure 1. (a) Schematic representation of the different selected systems (aqueous solution and ionic liquid-in-water, bicontinuous or water-in-ionic liquid microemulsions). (b) Chronoamperometric curves of the CoPt nanorods obtained at -1.05 V in (1) aqueous solution and (2) ionic liquid-in-water, (3) bicontinuous and (4) water-in-ionic liquid microemulsions in polycarbonate membranes. The currents are normalized by a geometrical area. (c) Deposition rate of CoPt in polycarbonate membranes and

conductivity of the deposition systems with respect to the aqueous percentage, on the same surfactant: ionic liquid ratio ($R_{S:IL}$=5.1).

Nanowires were synthesized potentiostatically, by applying a potential of -1.05 V and circulating a charge density of 9 C $cm^{-2}$ and by maintaining a semi-stirring regime (stirring with argon flow of the solution containing the membrane). As can be seen in the chronoamperometric curves (Figure 1b), the electrodeposition time necessary to circulate the same charge density is very different depending on the microemulsion structure, varying in the sense CoPt aqueous solution < IL/W microemulsion < β microemulsion < W/IL microemulsion. The deposition rate depends on the conductivity of the system (Figure 1c), which increases when the percentage of the CoPt aqueous solution in the microemulsion expands. However, the dependence deposition rate-conductivity is not linear and the structure of the microemulsion must also condition the deposition rate.

The composition of the CoPt nanorods synthesized in the four systems is practically constant ($Co_{33\pm2}Pt_{67\pm2}$). Therefore, in these semi-stirring conditions, the composition of the nanorods in a W/IL microemulsion does not replicate the relative proportion of Co and Pt in the aqueous component, as we observed in the non-stirring deposition of CoPt nanoparticles in a W/IL microemulsion [34, 35].

Although the composition is the same for the various CoPt nanorods, their morphology is different in each case. SEM and HRTEM pictures in Figure 2a show that compact nanowires are obtained in pure aqueous solution (W nanorods). However, the HRTEM pictures in Figures 2b-d show that all the nanowires obtained in the microemulsions (IL/W, β and W/IL nanorods) are porous. The diameters of the obtained nanorods ranged from 180 to 220 nm due to the non-uniformity of the nanochannels of the commercial polycarbonate membranes. The length of the nanorods, with the circulation of the same charge density, decreases from 4.1 μm for W, 3.7 μm for IL/W, 3.4 μm for β and 3.1 μm for W/IL nanorods, showing a decrease of the electrodeposition efficiency in the same direction as conductivity (Figure 1b). The average pore's size varies in the sense: IL/W > β > W/IL. IL/W nanorods showed a high degree of porosity, showing non-spherical pores ranging from 60 to 90 nm, which seemed larger than expected for the selected microemulsion system. Careful observation of Figure 2c confirmed that there were open mesoporous over the entire area forming a similar structure, as Figure 1a shows. Lastly, the maximum porosity and homogeneity was achieved by the nanorods obtained in the W/IL system, for

which small pores of 10-14 nm in diameter size, with a narrow pore size distribution, were observed. Therefore, the results demonstrate a successful preparation of different nano or mesoporous rods depending on the system structure, with a well-defined pore size along the nanorod.

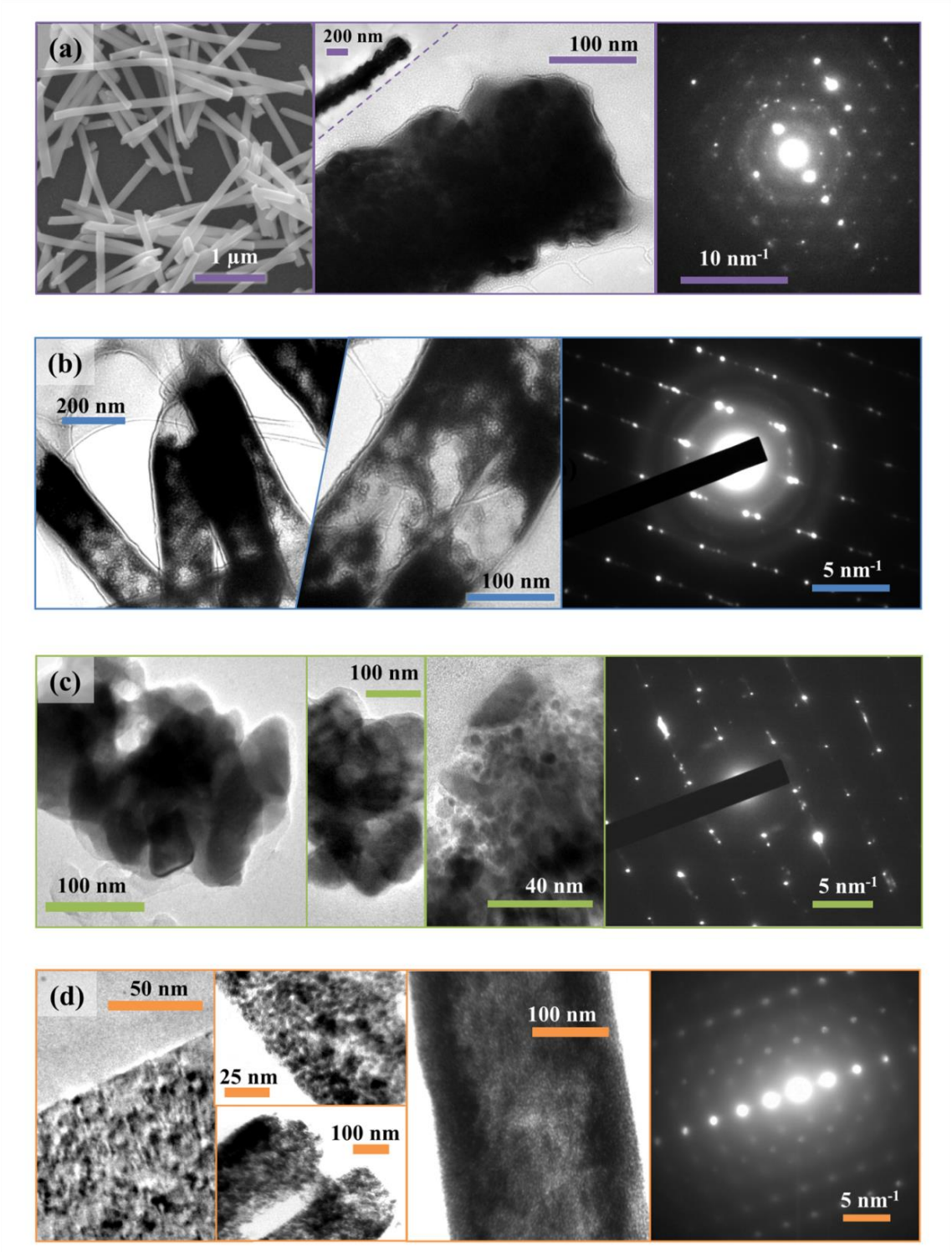

Figure 2. (a) SEM, HRTEM and SAED of W Nanorods. (b-d) HRTEM and SAED of IL/W (b), β (c) and W/IL (d) nanorods.

The Selected-Area Electron Diffraction patterns of the different nanorods can be indexed mainly as the (002), (101), (110) and (100) planes of a CoPt-hcp structure (strongly distorted Co-hcp structure). Moreover, some CoPt-fcc (slightly distorted Co-fcc structure) and cobalt oxide ($Co_3O_4$) planes were also detected [35,36]. However, the hcp:fcc ratio ($R_{hcp:fcc}$) increases as a result of the gradual decrease in the deposition rate from W/IL to W nanorods ($R_{hcp:fcc}$ W/IL> IL/W>β>W nanorods). A low deposition rate favours the formation of the hcp crystalline structure.

The electrocatalytic performance for methanol oxidation was evaluated in order to analyse the potentiality of our nanorods as a catalytic material. Figure 3a shows the CoPt loading mass-normalized cyclic voltammograms, corresponding to the first stabilization sweep, for all the CoPt nanorods in 0.5 M $H_2SO_4$ + 1 M methanol solutions. All the samples showed two anodic peaks during both the positive and negative sweep, which are typical of the methanol oxidation process. The ratio of the currents for the methanol oxidation from the forward scan ($j_f$) to the backward scan ($j_b$) is used to evaluate the poisoning tolerance of the catalysts towards the intermediate carbonaceous species accumulated on the electrode surface during the methanol oxidation in the direct methanol fuel cell [37-39]. The high $j_f/j_b$ values of all nanorods (Table 1) indicate their good poison tolerance, significantly improved compared with that of the commercial Pt/C catalysts. In addition, the methanol oxidation peaks corresponding to the nano or mesoporous CoPt nanorods clearly increase with respect to those obtained using the compact nanorods prepared in pure aqueous solution (W nanorods). The highest mass-normalized current densities of the W/IL nanorods (924 mA $mg^{-1}$ of CoPt), which is around 3.2, 3.5 and 9 times as high as that of IL/W, β and W nanorods, respectively, demonstrates the three-dimensional mesoporous network. Furthermore, the activity of the W/IL nanorods was also higher than that of the commercial Pt/C (around 250 mA $mg^{-1}$ in the same experimental conditions) or the state-of-the-art of Pt-base nanomaterials reported previously, such as mesoporous nanomaterials [15,16, 40-43], nanoplatelets and nanowires [44-46], Pt nanoparticles [47, 48] as well as other CoPt nanostructures [49-50].

Other parameters revealing the quality of the catalysts with respect to methanol oxidation are the onset potential of the oxidation process ($E_{onset}$) and the value of the mass-normalized current densities at 0.6 V ($j_{0.6V}$), which is the usual potential applied in the DMFCs. The onset potential significantly shifts to

negative values (Table 1), which indicates that our nano or mesoporous nanorods are more favourable for methanol oxidation than the non-porous CoPt nanorods or commercial Pt/C catalysts [37-40]. The specific activity at 0.6 V of the W/IL nanorods is the highest among the samples (Table 1), being 9 times as high as that of the non-porous nanorods. Then, a clear dependence of the catalyst efficiency on the structure and porosity grade of nanorods is observed.

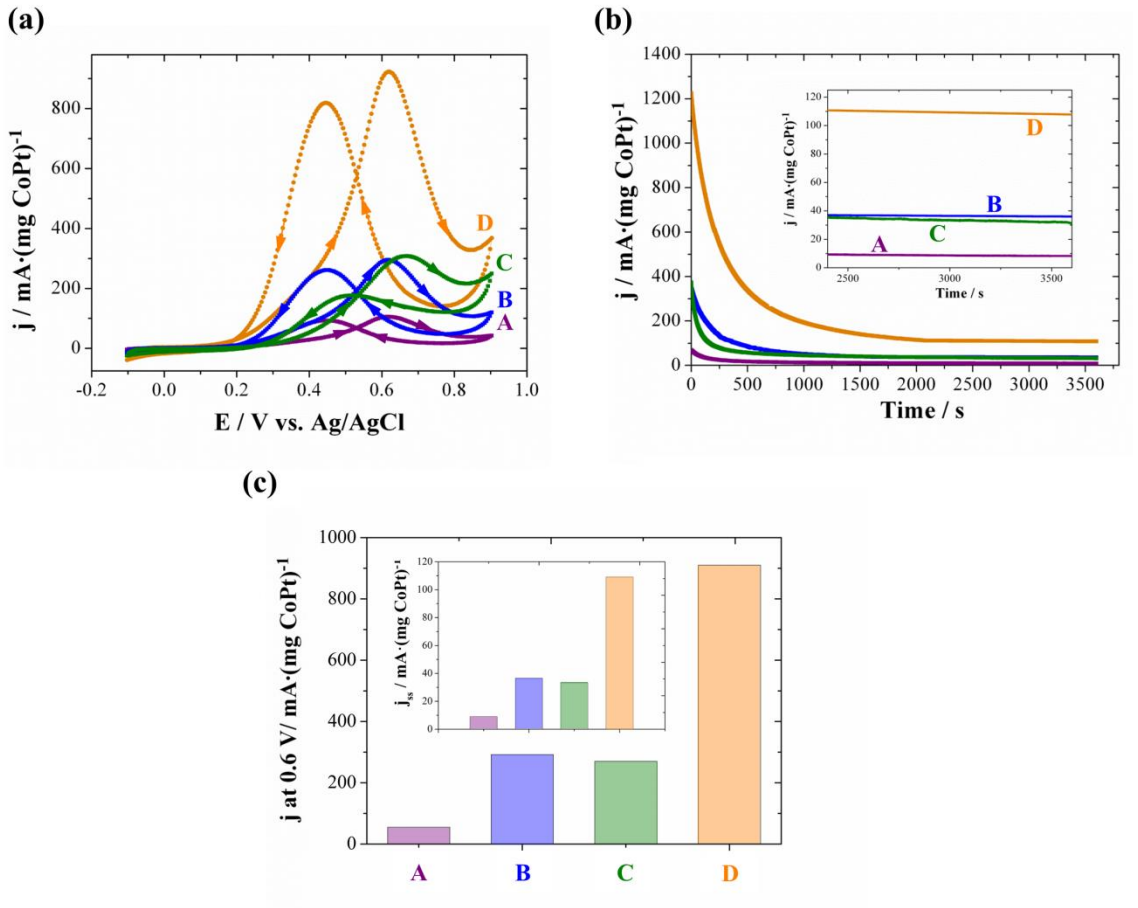


Figure 3. (a) Cyclic voltammograms (recorded at 50 mV $s^{-1}$) and (b) chronoamperometric curves (at 0.6 V) for methanol oxidation catalysed by (A) W, (B) IL/W, (C) β and (D) W/IL nanorods in 0.5 M $H_2SO_4$ containing 1M methanol. (c) Summary on the specific activities at 0.6 V and steady-state mass-normalized current density at 0.6 V (inset) for all the samples.

For a further evaluation of the electrocatalytic performance of all the CoPt nanorods, the chronoamperometric curves in 0.5 M $H_2SO_4$ + 1 M methanol solutions were recorded for 3600 s (Figure 3b). At short times, the samples show a rapid decay in the mass-normalized current densities, as a

consequence of the initial catalyst poisoning by intermediate species. However, the oxidation current decay on the W/IL nanorods is significantly slower than for the other nanowires. The W/IL nanorods maintain the steady-state mass-normalized current density ($j_{ss}$), which is 3.3 times as high as that of the other nano/mesoporous nanorods, and 12 times as high as that of the compact nanorods (Figure 3c). All the prepared nano/mesoporous electrocatalysts present a higher steady-state mass-normalized current density than that of the commercial Pt/C catalysts [37-40], thus demonstrating their enhanced electrocatalytic activity and stability.

The Electrochemically-active Surface Areas (ECSAs) of the nanorods were obtained by integrating the charge associated to the adsorption and desorption of hydrogen atoms in cyclic voltammograms recorded in 0.5 M of $H_2SO_4$ (Figure 4). The ESCA value is a critical parameter for defining the necessary CoPt nanorods loadings in the fuel cell application. Table 1 shows that logically, the ECSAs values, which are much larger for the W/IL nanorods, depend on their structure and porosity grade. The ESCA values also show that the porous architecture was well-developed even at the inner parts of the nanorods. The values of ECSA of our porous CoPt nanorods are higher than those of the mesoporous Pt nanorods, whereas the values of the compact CoPt are similar to those of the compact Pt nanorods [51-52].

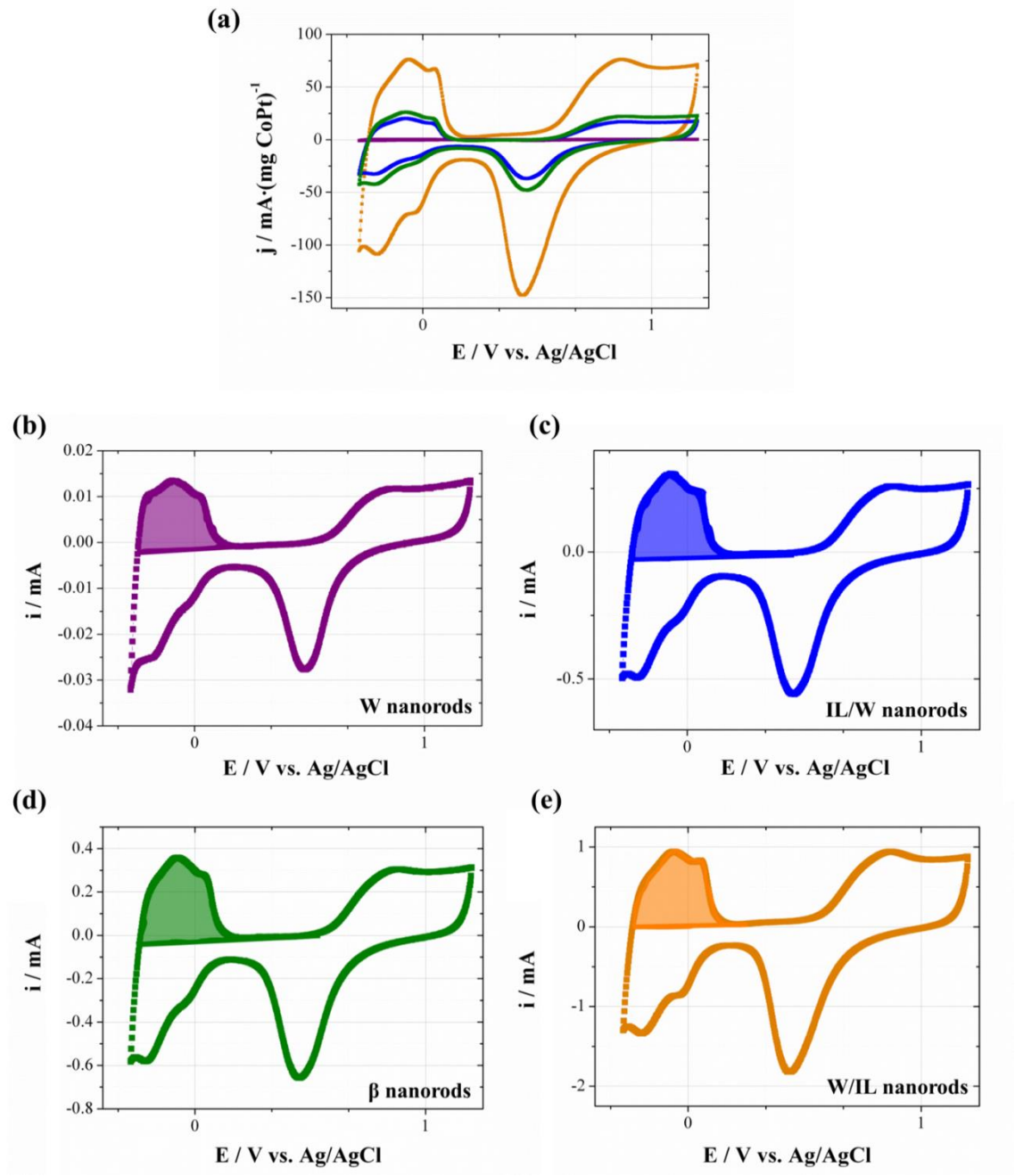


Figure 4. (a) Comparison of cyclic voltammetry curves for W, IL/W, β and W/IL nanorods recorded at room temperature in 0.5 M $H_2SO_4$ solution at a sweep rate of 100 mV $s^{-1}$. Cyclic voltammograms of (b) W, (c) IL/W, (d) β and (e) W/IL nanorods in 0.5 M $H_2SO_4$ solution. The ECSAs are estimated assuming the classic value to oxidize a mono-layer of hydrogen on bright Pt (210 μC·$cm^{-2}$) [53], although slight changes in this value have also been proposed [54].

We also investigated the effect of the nano or mesoporous nanostructure of the different synthesized nanorods, deposited by means of an ink (water and Nafion) on a Glassy Carbon electrode (GC), on the corrosion resistance of the nanostructures. The stability test of the electrocatalysts was carried out after immersing the samples until attaining the steady-state potential ($E_{ss}$) in a solution of NaCl (5 wt. %). Figure 5 shows the polarization curves, in a logarithmic scale, obtained by a linear potentiodynamic sweep from $E_{ss}$-300 to +300 mV at 0.1 mV $s^{-1}$. The values (shown in Table 1) of corrosion potential ($E_{corr}$) were positive, as expected for a Pt-containing alloy, and similar to those obtained for CoPt films of similar composition [55], which demonstrates the stability of the nanostructures supported in the Nafion ink. Surprisingly, a clear tendency was observed in the order W/IL> IL/W>β>W nanorods, which would be surprising due to the higher porosity of the W/IL nanorods with respect to that of the W ones. However, the higher corrosion stability of nano or mesoporous structures in comparison with compact nanorods can be justified by the different proportion of the hcp phase in each case ($R_{hcp:fcc}$) as, for similar composition of CoPt, the deposits showing hcp structure present a more positive corrosion potential than those with a fcc structure [55].

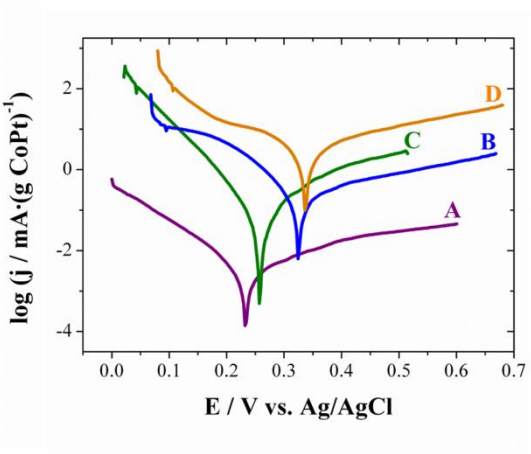


Figure 5. Potentiodynamic polarization curves in logarithmic scale corresponding to W (A), IL/W (B), β (C) and W/IL (D) nanorods in NaCl 5 % solution.

Table 1. Electrocatalysts characteristics.

| Nanorods system | ECSA / [$m^2 \cdot g^{-1}$] | $E_{onset}$ / [V] | $j_{0.6V}$ / [mA·(mg CoPt)$^{-1}$] | $j_f/j_b$ | $E_{cor}$ / [V] |
|---|---|---|---|---|---|
| W | 17.1 | 0.153 | 55.3 | 1.08 | 0.223 |
| IL/W | 45.4 | 0.055 | 291.8 | 1.11 | 0.325 |
| β | 64.8 | 0.151 | 270.1 | 1.74 | 0.256 |
| W/IL | 195.4 | 0.026 | 909.9 | 1.13 | 0.337 |

## 4. Conclusions

We successfully prepared different nano or mesoporous nanostructured CoPt nanorods by means of a facile electrochemical synthesis, at room-temperature (25 ºC), inside the channels of a commercial polycarbonate membrane, by using different microemulsions containing an ionic liquid. In all cases the nanorods prepared present in all cases high values of electrochemically-active surface areas, which depend on the nature of the microemulsion used. The present synthesis of porous nanowires has remarkable advantages in comparison with traditional or more recent proposals due to its versatility: the proposed method permits depositing nano or mesoporous nanorods of different metals or alloys using the described ionic liquid based microemulsions, by replacing the aqueous component of the microemulsion with any classical electrolytic bath containing the species to deposit.

In addition, the porous CoPt nanorods, especially the W/IL ones, exhibited high electrocatalytic activity for methanol oxidation and good corrosion resistance, along with a facile manipulation and recyclability by the anchoring or recovering due to their magnetic behaviour. They also showed a relatively good poison tolerance in the methanol oxidation, which makes them promising electrocatalysts for application in DMFCs.

**ACKNOWLEDGMENT**

Work supported by contract CQT2010-20726 from MINECO. Authors thank the CCiTUB for their equipment. A. S. would also like to thank the MIECD for its financial support (FPU Grant).

## AUTHOR INFORMATION

### Corresponding author

Prof. Elisa Vallés, Dr. (e.valles@ub.edu).

## References

[1] Xiang Q, Yu J, Jaroniec M, Synergetic effect of $MoS_2$ and graphene as cocatalysts for enhanced photocatalytic H2 production activity of $TiO_2$ nanoparticles. *J. Am. Chem. Soc*., 2012, **134**, 6575-6578.

[2] Wang L, Imura M, Yamauchi Y, Tailored Design of architecturally controlled pt nanoparticles with huge surface areas toward superior unsupported Pt electrocatalysts. *ACS Appl. Mater. Interfaces*, 2012, **4**, 2865-2869.

[3] Xiong H.-M, ZnO nanoparticles applied to bioimaging and drug delivery, *Adv. Mat.*, 2013, **25**, 5329-5335.

[4] Osberg K. D, Schumcker A. L, Sensei A. J, Mirkin C. A, One-dimensional nanorod arrays: independent control of composition, length, and interparticle spacing with nanometer precision, *Nano Lett.*, 2011, **11**, 820-824.

[5] Son Y. J, Kim H, Leong K. W, Yoo H.-S, Multifunctional nanorods serving as nanobridges to modulate T cell-mediated immunity, *ACS Nano*, 2013, **7**, 9771-9779.

[6] Huang X, El-Sayed I. H, Qian W, El-Sayed M. A, Cancer cell imaging and photothermal therapy in the near-infrared region by using gold nanorods, *J. Am. Chem. Soc.*, 2006, **128**, *2115-2120.*

[7] Aricò A. S, Bruce P, Scrosati B, Tarascon J.-M, Van Schalkwijk W, Nanostructured materials for advanced energy conversion and storage devices, *Nat. Mat.,* 2005, **4**, 366-377.

[8] Basri S, Kamarudin S. K., Daud W. R. W, Yaakub Z, nanocatalyst for direct methanol fuel cell (DMFC), *Int. J. Hydrogen Energy*, 2010, **35,** 7957-7970.

[9] Hsu C, Huang C, Hao Y, Liu F, Au/ Pd Shell nanoparticles for enhanced electrocatalytic activity and durability, *Electrochem. Commun.*, 2012, **23**, 133-136.

[10] Su L, Shrestha S, Zhang Z, Mustain W, Lei Y, Platinum- copper nanotube electrocatalyst with enhanced activity and durability for oxygen reduction reactions, *J. Phys. Chem. A*, 2013, **1**, 12293-12301.

[11] Zhao C, Li D, Feng Y, Size-controlled hydrothermal synthesis and high electrocatalytic performance of $CoS_2$ nanocatalysts as non-precious metal cathode materials for fuel cells, *J. Mater. Chem. A*, 2013, **1**, 5741-5746.

[12] Xiao L, Zhuang L, Liu Y, Lu J, Abruña H. D, Activating Pd by morphology tailoring for oxygen reduction, *J. Am. Chem. Soc*.,2009, **131**, 602-608.

[13] Kim T. W, Park I. D, Ryoo R, A Synthetic route to ordered mesoporous carbon materials with graphitic pore walls, *Angew. Chem. Int. Ed.*, 2003, **115**, 4511-4515.

[14] Joo H, Choi S. J, Oh I, Kwak J, Liu Z, Terasaki O, Ryoo R, Ordered nanoporous arrays of carbon supporting high dispersions of platinum nanoparticles, *Nature*, 2001, **412**, 169-172.

[15] Lee H. I, Stucky G. D, Kim J.H, Pak C, Chang H, Kim J.M, Spontaneous phase separation mediated synthesis of 3d mesoporous carbon with controllable cage and window size, *Adv. Mat*., 2011, **23**, 2357-2361.

[16] Chu W.-C, Li J.-G, Kuo S.-W, From flexible to mesoporous polybenzoxazine resins templated by poly(ethylene oxide-*b*-ε-caprolactone) copolymer through reaction induced microphase separation mechanism, *RSC Adv.*, 2013, **3**, 6485-6498.

[17] Cherevko S, Kulyk N, Chung C.-H, Pulse-reverse electrodeposition for mesoporous metal films: combination of hydrogen evolution assisted deposition and electrochemical dealloying, *Nanoscale*, 2012, **4**, 568-575.

[18] Xu C, Li Y, Tian F, Ding Y, Dealloying to nanoporous silver and its implementation as a template material for construction of nanotubular mesoporous bimetallic nanostructures, *ChemPhysChem*, 2010, **11**, 3320-3328.

[19] Köhler C, Kloke A, Drzyzga A, Zengerle R, Kerzenmacher S, Fabrication of highly porous platinum electrodes for micro-scale applications by pulsed electrodeposition and dealloying, *J. Power Sources*, 2013, **242**, 255-263.

[20] Dickinson C, Zhou W, Hodgkins R. P, Shi Y, Zho D, He H, Formation mechanism of porous single-crystal $Cr_2O_3$ and $Co_3O_4$ templated by mesoporous silica, *Chem. Mater.*, 2006, **18**, 308.

[21] Wang D, Luo H, Kou R, Gil M. P, Xiao S, Colub V. O, Yang Z, Brinker C. J, Lu Y, A general route to macroscopic hierarchical 3D nanowire networks, *Angew. Chem. Int. Ed.*, 2004, **116**, 6295-6299.

[22] Yamauchi Y, Tonegawa A, Komatsu M, Wang H, Wang L, Nemoto Y, Suzuki N, Kuroda K, Electrochemical synthesis of mesoporous Pt–Au binary alloys with tunable compositions for enhancement of electrochemical performance, *J. Am. Chem. Soc.*, 2012, **134**, 5100-5109.

[23] Chen Y, Chen H, Guo L, He Q, Chen F, Zhou J, Feng J, Shi J, Hollow/rattle-type mesoporous nanostructures by a structural difference-based selective etching strategy, *ACS Nano*, 2010, **4**, 529-539.

[24] Li C, Sato T, Yamauchi Y, Electrochemical synthesis of one-dimensional mesoporous Pt nanorods using the assembly of surfactant micelles in confined space, *Angew. Chem. Int. Ed.*, 2013, **125**, 8208-8211.

[25] Antolini E, Salgado J. R. C, Gonzalez E. R, The methanol oxidation reaction on platinum alloys with the first row transition metals: the case of Pt-Co and Pt-Ni alloy electrocatalysts for DMFCs: a short review, *Appl.Catal. B* 2006, **63**, 137-149.

[26] Ding L.-X, Li G.-R, Wang Z.-L, Liu Z.-Q, Liu H, Tong Y.-X, Porous Ni@Pt core-shell nanotube array electrocatalyst with high activity and stability for methanol oxidation, *Chem.-Eur. J.*, 2012, **18**, *8386-8391*.

[27] Long J. F, Logan M. S, Rhodes C. P, Carpenter E. E, Stroud R. M, Rolison D. R, Nanocrystalline iron oxide aerogels as mesoporous magnetic architectures, *J. Am. Chem.Soc.*, 2004, **126**, 16879-16889.

[28] Hu M, Jiangand J. S, Zeng Y, Prussian blue microcrystals prepared by selective etching and their conversion to mesoporous magnetic iron(III) oxides, *Chem. Commun.*, 2010, **46,**1133-1135.

[29] Das B, Mandal M, Mandal K, Sen P, Influence of alumina membrane on magnetic properties for thermally annealed CoPt alloy nanowires, *Colloid. Surface A*, 2014, **443**, 398-403.

[30] Wen X, Zhang X. X, Zhang Y, Yue G. H, Wang J. B, Wang Z. W, Peng D. L, Structure and magnetic properties of the $Co_x Pt_{100-x}$ nanowire arrays, *Appl. Phys.*, 2013, **112,** 869-875.

[31] Cao M, Wu D, Cao R, Recent advances in the stabilization of platinum electrocatalysts for fuel-cell reactions, *ChemCatChem.* 2014, **6**, 26-45.

[32] Antolini E, Salgado J. R. C, Gonzalez E. R, The stability of Pt–M (M = first row transition metal) alloy catalysts and its effect on the activity in low temperature fuel cells. A literature review and tests on a Pt–Co catalyst, *J. Power Sources*, 2006, **160**, 957-968.

[33] Gao Y, Han S, Han B, Li G, Shen D, Li Z, Du J, Hou W, Zhang G, TX-100/water/1-butyl-3-methylimidazolium hexafluorophosphate microemulsions, *Langmuir*, 2005, **21**, 5681-5684.

[34] Serrà A, Gómez E, López-Barbera J. F, Nogués J. Vallés E, Green electrochemical template synthesis of CoPt nanoparticles with tunable size, composition, and magnetism from microemulsions using an ionic liquid ($bmimPF_6$), *ACS Nano*, 2014, **8**, 4630-4639.

[35] Serrà A, Gómez E, Vallés E, One-step electrodeposition from ionic liquid and water as a new method for 2D composite preparation, *Electrochem. Commun.*, 2014, **46**, 79-83.

[36] Serrà A, Gómez E, Vallés E, Electrosynthesis method of CoPt nanoparticles in percolated microemulsions, *RSC Adv*. 2014, **4**, 34281-334287.

[37] Gasteiger H. A, Kocha S. S, Sompalli B, Wagner F. T, Activity benchmarks and requirements for Pt, Pt-alloy, and non-Pt oxygen reduction catalysts for PEMFCs, *Appl. Catal., B,* 2005, **56**, 9-35.

[38] Liu Y.-T, Yuan Q.-B, Duan D.-H, Zhang D.-H, Hao X.-G, Wei G.-Q, Liu S.-B, Electrochemical activity and stability of core–shell $Fe_2O_3$/Pt nanoparticles for methanol oxidation, *J. Power Sources,* 2013, **243**, 622-629.

[39] Sahim O, Kivrak H, A comparative study of electrochemical methods on Pt–Ru DMFC anode catalysts: The effect of Ru addition, *Int. J. Hydrogen Energ.*, 2013, **38**, 901-909.

[40] Li C, Jiang B, Imura M, Malgras V, Yamauchi Y, Mesoporous Pt hollow cubes with controlled shell thicknesses and investigation of their electrocatalytic performance, *Chem. Commun.,* 2014, **50**, 15337-15340.

[41] Ding L.-X, Li G.-R, Wang Z.-L, Liu Z.-Q, Liu H, Tong Y.-X, Porous Ni@Pt Core-Shell Nanotube Array Electrocatalyst with High Activity and Stability for Methanol Oxidation, *Chem.-Eur. J.*, 2012, **18**, 8386-8391.

[42] Liu L, Pippel E, Scholz R, Gosele U, Nanoporous Pt−Co alloy nanowires: fabrication, characterization, and electrocatalytic properties, *Nano Lett.,* **2009**, *4, 4352-4358.*

[43] Ma C, Kang L, Shi M, Lang X, Jiang Y, Preparation of Pt-mesoporous tungsten carbide/carbon composites via a soft-template method for electrochemical methanol oxidation, *J. Alloy. Compd.,* 2014, **588**, 481-487.

[44] Li H.-H, Zhao S, Gong M, Cui C.-H, He D, Liang H.-W, Wu L, Yu S.-H, Ultrathin PtPdTe nanowires as superior catalysts for methanol electrooxidation, *Angew. Chem. Int. Ed.*, 2013, **52**, 7472-7476.

[45] Luo B, Yan X, Xu S, Xue Q, Synthesis of worm-like PtCo nanotubes for methanol oxidation, *Electrochem. Commun.*, 2013, **30**, 71-74.

[46] Hong W, Wang J, Wang E, Dendritic Au/Pt and Au/PtCu nanowires with enhanced electrocatalytic activity for methanol electrooxidation, *Small*, 2014, **10**, 3262-3265.

[47] Okamoto M, Fujigaya T, Nakashima N, Design of an assembly of poly(benzimidazole), carbon nanotubes, and pt nanoparticles for a fuel-cell electrocatalyst with an ideal interfacial nanostructure, *Small*, 2009, **5**, 735-740.

[48] Bai L, Zhu H, Thrasher J. S, Street S.C, Synthesis and electrocatalytic activity of photoreduced platinum nanoparticles in a poly(ethylenimine) matrix, *ACS Appl. Mater. Interfaces*, 2009**, 1**, 2304-2311.

[49] Xu J, Liu X, Chen Y, Zhou Y, Lu T, Tang Y, Platinum-Cobalt alloy networks for methanol oxidation electrocatalysis, *J. Mater. Chem.*, 2012, **22**, 23659-23667.

[50] Zheng J-N, He L-L, Chen C, Wang A-J, Ma K-F, Feng J-J, One-pot synthesis of platinum$_3$cobalt nanoflowers with enhanced oxygen reduction and methanol oxidation, *J. Power Sources*, 2014, **268**, 744-751.

[51] Cortés M, Gómez E, Vallés E, Magnetic properties of nanocrystalline CoPt electrodeposited films. Influence of P incorporation, *J. Solid State Electr.*, 2010, **14**, 2225-2233.

[52] Khudhayer W. J, Kariuki N. N, Wang X, Myers D. J, Shaikh A. U, Karabacak T, Oxygen reduction reaction electctrocatalytic activity of glancing angle deposited platinum nanorod arrays, *J. Electrochem. Soc.*, 2011, **158**, 1029-1041.

[53] Trasatti S, Petrii O. A, Real surface area measurements in electrochemistry, *Pure Appl. Chem.*, 1991, **63**, 711-734.

[54] Chen Q.-S, Solla-Gullón J, Sun S.-G, Feliu J. M, The potential of zero total charge of Pt nanoparticles and polycrystalline electrodes with different surface structure: The role of anion adsorption in fundamental electrocatalysis, *Electrochim. Acta*, 2010, **55**, 7982-7994.

[55] Cortés M, Serrà A, Gómez E, Vallés E, CoPt nanoscale structures with different geometry prepared by electrodeposition for modulation of their magnetic properties, *Electrochim. Acta*, 2001, **56**, 8232-8238.